



Shikonin improves the effectiveness of PD-1 blockade in colorectal cancer by enhancing immunogenicity via Hsp70 upregulation

Jinghua Chen^{1,2} · Jie Liu³ · Xiaolin Liu² · Jun Wang² · Xiumei Wang⁴ · Xin Ye² · Qi Xie² · Jing Liang² · Yan Li^{1,2}

Received: 16 May 2023 / Accepted: 23 October 2023 / Published online: 6 January 2024
© The Author(s) 2024

Abstract

Background PD-1 blockade has shown impressive clinical outcomes in colorectal cancers patients with high microsatellite instability (MSI-H). However, the majority of patients with colorectal cancer who present low microsatellite instability (MSI-L) or stable microsatellites (MSS) show little response to PD-1 blockade therapy. Here, we have demonstrated that Shikonin (SK) could induce cell death of CT26 cells via classically programmed and immunogenic pathways.

Methods and results SK promoted the membrane exposure of calreticulin and upregulated the expression of heat shock protein 70 (Hsp70). The upregulation of Hsp70 was dependent on ROS induced by SK and silencing of PKM2 in CT26 cells reverts ROS upregulation. Besides, SK synergizes with PD-1 blockade in CT26 tumor mice model, with the increase of intramural DC cells and CD8⁺ T cells. The expression of Hsp70 in tumor tissue was also increased in combinational SK plus α PD-1 therapy group.

Conclusions Our study elucidated the potential role of ‘Shikonin-PKM2-ROS-Hsp70’ axis in the promotion of efficacy of PD-1 blockade in CRC treatments, providing a potential strategy and targets for improving the efficacy of PD-1 blockade in colorectal cancer.

Keywords Shikonin · PD-1 blockade · Colorectal cancer · Hsp70 · Stable microsatellites

Introduction

Colorectal cancer (CRC) is the most common digestive tract tumor, accounting for approximately 9.7% of all cancer patients and approximately 8.5% of tumor-related deaths [1]. The standard treatment for metastatic CRC is chemotherapy combined with targeted therapy, such as anti-angiogenic agents (ramucirumab, bevacizumab or aflibercept) or anti-EGFR drugs (cetuximab or panitumumab) for patients with RAS wild-type [2, 3]. However, in cases where these common treatments fail, treatment options are limited. In recent years, immunotherapy for cancer has made great progress. Among these advances, PD-1 blockade has elicited promising clinical response in a variety of solid tumors, including melanoma and non-small cell lung cancer [4, 5]. However, only 5% patients with microsatellite instability-high (MSI-H)/deficient mismatch repair (dMMR) CRC could benefit from PD-1 blockade therapy [6, 7]. For the larger subgroup of non-MSI-H/dMMR CRC patients, combined regimens are strongly needed and might be an ideal strategy to address the conundrum [8].

✉ Qi Xie
xieqi@sdfmu.edu.cn

✉ Jing Liang
liangjing0531@163.com

✉ Yan Li
liyan16766@163.com

¹ Shandong Provincial Qianfoshan Hospital, Shandong University, Jinan, China

² Shandong Key Laboratory of Rheumatic Disease and Translational Medicine, Department of Oncology, Shandong Lung Cancer Institute, The First Affiliated Hospital of Shandong First Medical University & Shandong Provincial Qianfoshan Hospital, Jinan, China

³ Department of Pediatric Intensive Care Unit, Shandong Provincial Maternal and Child Health Care Hospital Affiliated to Qingdao University, Jinan, China

⁴ Department of Oncology, The Yuncheng Chenxin Hospital, Heze, China

Damage-associated molecular patterns (DAMPs) are endogenous molecules released from damaged or dying tumor cells, and they have been shown to activate the innate immune system by interacting with innate receptors [9]. DAMPs could modulate the tumor immune microenvironment (TIME) and influence tumor growth. Immunogenic cell death (ICD), is a form of cell death which activates adaptive immunity and induces long-term immune memory [10]. ICD could be induced by endoplasmic reticulum (ER) stress and reactive oxygen species (ROS) generation, which leads to release of DAMPs [11–13].

Shikonin (SK) is the bioactive purplish red naphthoquinone extracted from the natural plant Zongfu root [14]. Some researchers have found that SK could induce apoptosis of colon cancer cells, and regulate invasion and autophagy [15, 16]. SK has also been proved to be an inducer of ROS in tumor cells, whereby inducing apoptosis and release of DAMPs [17]. Lin et al. has found that Shikonin can enhance the cellular immunogenicity of tumor vaccines through different DAMPs. Among three DAMPs tested, they found that the Hsp70 is the most important component in facilitating DC immunity on inhibiting metastasis of mouse tumors and prolonging mouse survival [18]. However, the complete understanding of the mechanism behind Hsp70 upregulation induced by Shikonin is still under investigation. Chen et al. has found that SK could induce ICD of melanoma B16 cells and enhance function of dendritic cells (DCs) [19]. Previous studies have confirmed that SK and BET inhibitor JQ1 can synergistically exert anti-tumor effects by reshaping the tumor immune microenvironment [20]. However, there is limited research available on the effects of combining shikonin (SK) and PD-1 blockade for the treatment of CRC. Further studies are required to explore the potential benefits and mechanisms of this combination therapy. In the present study, we investigated the effect of SK combined with α PD-1 therapy in CT26 tumor model, which is known to be microsatellite stability (MSS). In addition, we investigated the synergistic mechanism of combining SK with α PD-1 by examining the effects on apoptosis, release of DAMPs, and changes in the tumor immune environment. Our study demonstrated a theoretical basis for SK combined α PD-1, providing a potential treatment strategy for CRC who could not benefit from PD-1 blockade.

Materials and methods

Chemicals, reagents and antibodies

Shikonin was purchased from Sigma-Aldrich (Cat No. 517-89-5, St. Louis, MO, USA). Purified anti-mouse PD-1 (clone RMP1-14) was purchased from BioXcell (Cat No. BE0146, West Lebanon, NH, USA). Fluorescent-labeled anti-mouse

CD4 antibody (Cat No. 100406), anti-CD8 antibody (Cat No. 301014), anti-CD11b antibody (Cat No. 101212), anti-CD11c antibody (Cat No. 117308) were purchased from Biolegend (San Diego, CA, USA). Anti-mouse calreticulin antibody (Cat No. ab92516) and anti-mouse Hsp70 antibody (Cat No. ab181606) were purchased from Abcam (Cambridge, UK). 7-AAD Viability Staining Solution was purchased from Invitrogen (Cat No. 00-6993, Waltham, MA, USA). Acetylcysteine was purchased from MCE (Cat No. HY-B0215, NJ, USA). 2,7-Dichlorodihydrofluorescein was purchased from APEXbio (Cat No. C3890, Houston, TX, USA).

Cell

CT26 cells were obtained from the cell bank of the Chinese Academy of Sciences (Shanghai, China) and cultured in RPMI1640 containing 10% FBS at 37 °C and 5% CO₂ condition.

Mice

20 SPF female BALB/c mice (6–8 weeks old, weight 16–19 g) were purchased from Beijing Vital River Laboratory Animal Technology Co., Ltd. All animal experiment has been approved by the Ethics Committee of the first affiliated Hospital of Shandong first Medical University. All mice were exposed to ambient humidity of 60% and temperature of 20–26 °C to ensure a 12 h light cycle every day.

In vivo CT26 tumor mouse model

6×10^5 CT26 cells were subcutaneously inoculated into BALB/c mice in the right inguinal region. The tumor volume was calculated as $0.5 \times \text{length} \times \text{width}^2$. Tumor-bearing mice were randomized into 4 groups: Group A: IgG (n=5); Group B: IgG + SK (n=5); Group C: anti-PD-1 mAb (n=5); Group D: anti-PD-1 mAb + SK (n=5). Mice were given drugs when the tumor volume grew to about 62.5 mm³. SK was intraperitoneally injected at 3 mg/kg every 2 days for a total of seven times [17, 21, 22], and the same volume of DMSO was given to group A and group C as control for SK. Anti-PD-1 antibody was intraperitoneally injected at 50 μ g/mice on the 5th and 9th day [23, 24], and the same volume of IgG was given to group A and group B as control for α PD-1. On the 16th day, the mice were sacrificed and the volume of tumor was measured.

Apoptosis analysis

CT26 cells seeded in six-well plates (4×10^5 cells/well) were treated with DMSO, SK (5 μ M or 10 μ M) for 24 h, and then cells were harvested, washed twice with ice-cold PBS,

stained with Alexa Fluor 488-Annexin V and 7-AAD for 15 min at room temperature in the dark, and then analyzed by using flow cytometry.

ROS generation

CT26 cells were seeded in six-well plates (4×10^5 cells/well) and treated with DMSO, SK (5 μ M or 10 μ M), NAC (10 mM) for 24 h. NAC was given 2 h before SK treatments, and cells were incubated with 10 μ M H₂DCFDA for 40 min in 37°C cell incubator [25]. ROS expression in cells were analyzed by fluorescence microscope.

CRT exposure analysis

CT26 cells seeded in six-well plates (4×10^5 cells/well) were cultured with DMSO, SK (5 μ M or 10 μ M) for 24 h. The treated cells were collected, incubated with Alexa Fluor 488-anti mouse CRT antibody for 30 min at room temperature in the dark, and analyzed by flow cytometer to identify CRT exposure.

CRT, HMGB1 and Hsp70 expression analysis

Tumor cell lysate samples were prepared as previously described [19]. The protein samples were resolved by SDS-PAGE using 10 or 15% stepwise gels. The resolved proteins were transferred to a PVDF membrane, and the membrane was blocked with 5% non-fat dry milk in TBST buffer for 60 min at room temperature. The membranes were incubated with primary antibodies (1:1000 dilutions) overnight at 4 °C, and then with HRP-conjugated secondary antibody (1:8000 dilutions) for 1 h at room temperature and washed with TBST buffer. The transferred proteins were visualized with an enhanced chemiluminescence (ECL) detection assay kit. Quantification of bands was performed using Image J software (National Institutes of Health, Bethesda, Md, USA).

Transfection

According to the manufacturers' protocol, all the small interfering RNAs (siRNAs) including siRNA-pyruvate kinase M2 and negative control siRNA (si-NC) (GenePharma) were transfected into CT26 cells using the Lipofectamine 3000 Reagent (Invitrogen). The silencing effect was confirmed by western blotting.

Statistical analysis

Each experiment was performed on at least three separate occasions and the number of independent experiments carried out are stated in figure legends. Statistical analyses

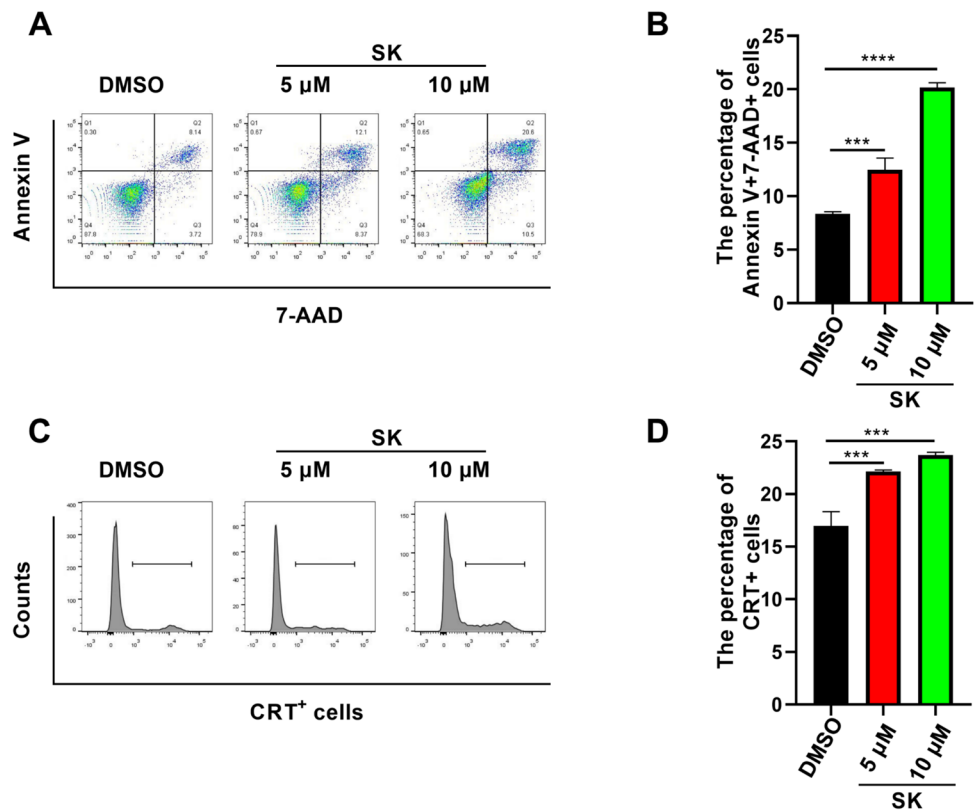
were performed using SPSS 19.0 (IBM, Armonk, NY, USA). Data that conform to the normal distribution are presented as the mean \pm standard deviation (SD). *t* test was used to determine the statistical significance of differences between two variables. A one-way analysis of variance (ANOVA) test was used for statistical comparisons between groups (when number of groups are more than 3). *P* < 0.05 was considered statistically significant. Prism version 6 (GraphPad Software Inc., San Diego, CA, USA) was used for graphic presentation.

Results

CT26 cell death was induced by Shikonin via classically programmed and immunogenic pathways

To evaluate anti-tumor effects of SK on colorectal cancer cells, CT26 cells, the murine colorectal carcinoma cell line, were treated with SK at different concentrations. The apoptosis rate of CT26 cells was detected using flow cytometry. Compared with control group ($8.36 \pm 0.193\%$), the percentage of Annexin V⁺ 7-ADD⁺ cells after SK treatments (5 μ M) was increased ($12.47 \pm 1.097\%$) (*P* < 0.001), while further been increased to $20.17 \pm 0.451\%$ at high SK concentration (10 μ M, *P* < 0.0001) (Fig. 1A, B), indicating that SK significantly induced apoptosis of CT26 cells in a dose-dependent manner. Meanwhile, in order to figure out whether SK induces immunogenic cell death (ICD), three DAMPs expressions on CT26 cells were determined. In terms of CRT cell-surface exposure, we found that SK at 5 μ M ($22.13 \pm 0.153\%$) (*P* < 0.001) and 10 μ M ($23.70 \pm 0.265\%$) (*P* < 0.001) both effectively enhance CRT cell-surface exposure compared with DMSO ($16.97 \pm 1.350\%$) (Fig. 1C, D). Furthermore, the expressions of CRT, HMGB1 and Hsp70 in CT26 cells treated with SK were quantified by western blotting. In comparison with control group, there was no significant expression change of CRT and HMGB1 after SK treatments (Fig. 2A), and the expression of soluble HMGB1 determined by ELISA was not significantly changed (Data not shown). However, SK induced upregulation of Hsp70 in CT26 cells in a dose-dependent manner (*P* < 0.05) (Fig. 2A, D). The inconsistent results obtained from flow cytometry and Western blotting for CRT suggest that SK only aids in the movement of CRT from its intracellular compartments to the surface of the cell, without actually increasing the overall expression of the protein. The above results indicated that SK significantly induced cell death of CT26 cells via the classically programmed and immunogenic pathway.

Fig. 1 CT26 cell death was induced by Shikonin via classically programmed and immunogenic pathways. CT26 cells were treated with SK (5 μ M or 10 μ M) for 24 h and then cell apoptosis was determined. **A** Cells were stained by Annexin V and 7-AAD and were analyzed by flow cytometry. **B** The percentage of Annexin V+ and 7-AAD+ cells are shown. **C** CRT cell surface expression upon treatment with SK were determined by flow cytometry. **D** The percentage of CRT+ cells are shown. Data are expressed as mean \pm SD of three independent experiments. *** P < 0.001; **** P < 0.0001.



Shikonin-induced Hsp70 upregulation was dependent on increased reactive oxygen species

Previous studies have reported that ROS can regulate the activity and expression of Hsp70 by activating certain oxidative-reduction signaling pathways [26]. To explore the potential mechanisms of Hsp70 upregulation on CT26 cells induced by SK, we investigated whether SK affect ROS production in CT26 cells. Our results showed that both SK at 5 μ M and 10 μ M significantly induced ROS generation in CT26 cells compared with DMSO control. In order to assure the inductive effect of ROS in the increase of Hsp70 expression, N-acetyl-L-cysteine (NAC), a ROS inhibitor, was employed in blocking experiment. As expected, NAC significantly inhibited SK-induced ROS accumulation at different concentrations (Fig. 3A). Of note, NAC significantly abolished the upregulation of Hsp70 induced by SK in CT26 cells (Fig. 3B, C), suggesting that the increase of Hsp70 expression induced by SK was dependent on SK-induced ROS in CT26 cells.

Silencing of PKM2 in CT26 cells reverts ROS upregulation induced by Shikonin

It has been reported that pyruvate kinase M2 (PKM2), a glycolytic enzyme that play a critical role in aerobic glycolysis

and cell growth, was increased in colorectal cancer, promoting proliferation and migration of colon cancer cells [27, 28]. Shikonin has been regarded as the effective inhibitor of PKM2 [29]. In order to clarify whether SK induced ROS in a PKM2-dependent manner, we silenced PKM2 gene expression in CT26 cells using PKM2-siRNA and determine ROS production after SK treatments. Compared with siRNA NC control, silencing of PKM2 significantly reduced the production of ROS induced by SK (Fig. 4A, B). This result indicates that increased ROS was induced by SK in a PKM2-dependent manner.

Shikonin synergizes with PD-1 blockade in CT26 tumor mice model

It has been reported that chemotherapy drugs could improve the efficacy of PD-1 blockade in colorectal cancer treatment by triggering DAMPs release [30]. Since SK could induce DAMPs release, we tested whether there is any synergistic effect in combinational SK and PD-1 blockade therapy. For this purpose, CT26-bearing mice were established and treated with SK, α PD-1 or SK plus α PD-1. Mice received SK and α PD-1 treatments have shown smaller tumors volume ($294.1 \pm 231.2 \text{ mm}^3$) compared to mice receiving α PD-1 monotherapy ($489.2 \pm 444.6 \text{ mm}^3$) ($P < 0.0001$) or IgG control group ($1048 \pm 1016 \text{ mm}^3$) ($P < 0.0001$) (Fig. 5), suggest

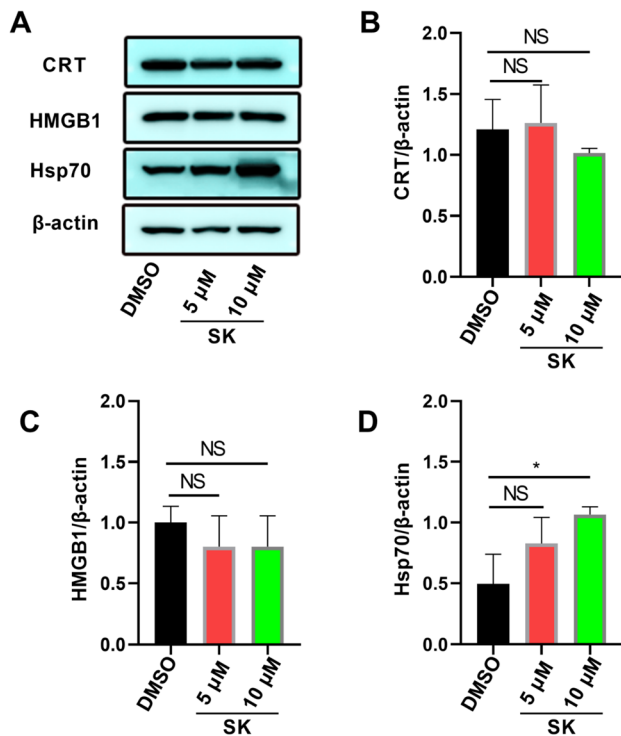


Fig. 2 SK induced-ICD makers of CT26. CT26 cells were treated with SK (5 μ M or 10 μ M) for 24 h. **A** The expression of CRT, HMGB1 or Hsp70 in CT26 cells was determined using western blotting. **B–D** β -actin was used as a loading control and the ratio of target protein to β -actin was shown. Data are expressed as mean \pm SD of three independent experiments. * $P < 0.05$

that SK synergizes with PD-1 blockade in CT26 tumor mice model.

Combinational Shikonin and PD-1 blockade modified tumor immune-microenvironment

In order to explore the cellular and molecular mechanism underlying the synergetic effect of α PD-1 and SK, immune-microenvironment in solid tumor was evaluated and the percentage of DC or T cells was determined by using flow cytometry. As shown in Fig. 6, combination of SK and α PD-1 treatments significantly increased infiltration of intratumoral CD8⁺ T cells (SK + α PD-1: $2.52 \pm 0.659\%$, α PD-1: $1.600 \pm 0.501\%$) (Fig. 6A, B). Also combinational therapy induced a trend of increased the percentages of CD11c⁺CD11b⁺ DC cells ($4.02 \pm 2.112\%$) when compared to α PD-1 monotherapy ($2.63 \pm 0.538\%$) (Fig. 6C, D). Immunohistochemistry has been to confirm more intratumoral CD8⁺ T cells after combination of SK and α PD-1 treatments (0.27 ± 0.045) compared with IgG control (0.07 ± 0.051) ($P < 0.001$) or α PD-1 monotherapy (0.14 ± 0.026) ($P < 0.05$) (Fig. 6E, F). In addition, we found that the expression of Hsp70 in tumor tissue was significantly increased after

SK and α PD-1 treatments (32.61 ± 11.260) compared with IgG control (7.14 ± 4.772) ($P < 0.05$) or α PD-1 alone (7.98 ± 6.519) ($P < 0.05$) (Fig. 7A, B). Above all, these results indicated SK and α PD-1 treatments modified tumor immune-microenvironment with the change of percentage of immune cells and expression of Hsp70.

Discussion

In this study, we have found that Shikonin (SK) could synergize with PD-1 blockade in CT26 tumor model, along with increased DC cells and CD8⁺ T cells. CT26 cell death was induced by SK via classically programmed and immunogenic pathways. Among all DAMPs, SK specifically induced Hsp70 upregulation dependent on increased ROS, whilst silencing of PKM2 in CT26 cells reverts ROS upregulation. Our study elucidated the potential role of ‘Shikonin-PKM2-ROS-Hsp70’ axis in the promotion of efficacy of PD-1 blockade in CRC treatments (Fig. 7C).

Immune checkpoints inhibitor, α PD-1, is highly effective in patients with advanced melanoma, non-small cell lung cancer or metastatic renal cell carcinoma [31–33]. However, PD-1 blockade has been considered as the ineffective therapy in most CRC patients, except for those with MSI-H or high mutational burden. Thus, it is necessary to improve the efficacy of PD-1 blockade, and combinational therapy has been as the popular options. For the first time, we found that Shikonin could synergize with PD-1 blockade in CT26 tumor model, providing potential therapy regimen for patients with MSS CRC.

Our findings those combinational SK and PD-1 blockade modified tumor immune-microenvironment were consistent with other researchers. Lin et al. have demonstrated Shikonin effectively upregulated Hsp70 and CRT expressions, but not HMGB1 in 4T1 cells. They also found that CRT and Hsp70 mediated a critical role in Shikonin-treated 4T1 cell lysates-induced DC cell immunity, with significant CD4⁺ and CD8⁺ T cell proliferation. Besides, Hsp70 is regarded as the most critical component in enhancing DC immunity on suppressing tumor metastasis [18]. In our study, the upregulation of Hsp70 in tumor tissue was also observed after SK and PD-1 blockade treatments. Chen et al. concluded that Shikonin could effectively increase the production of specific DAMPs in B16 cells, including Hsp70, Hsp90, CRT and HMGB1. Shikonin-treated B16 cell lysates could induce DCs to a higher level of functional and phenotypic maturation, exhibiting high expression of CD86 and MHC class II and Th1 cells activation [19]. In our study, we also found that the percentage of CD11⁺CD11b⁺ DC and CD8⁺ T cells have been increased, suggesting that synergistic effect of SK with PD-1 blockade in CT26 tumor mice model might due to DC activation and cytotoxic CD8⁺ T cells infiltration.

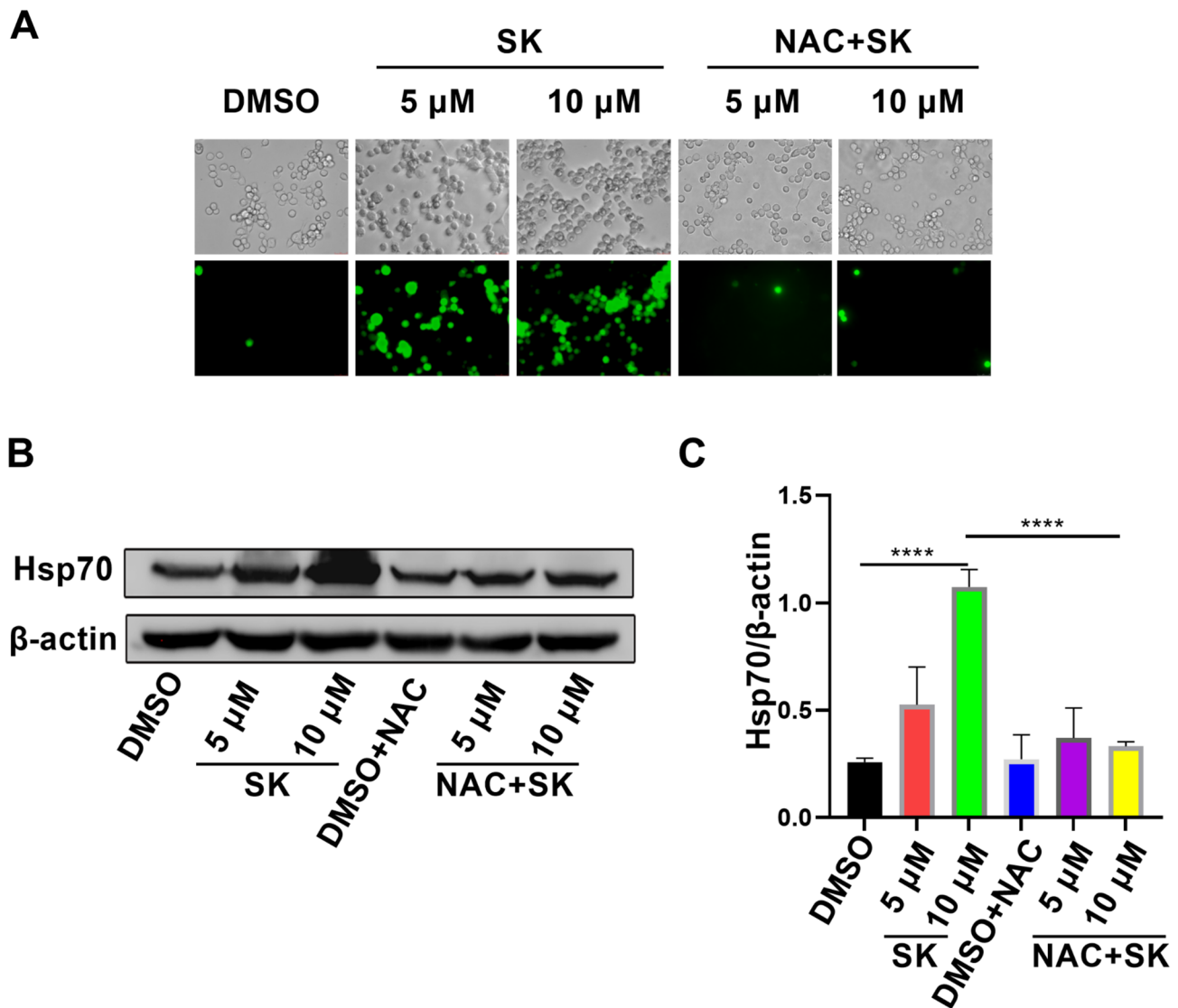


Fig. 3 Shikonin-induced Hsp70 upregulation was dependent on increased reactive oxygen species. CT26 cells were incubated with SK (5 μ M or 10 μ M) or/and NAC (10 mM) for 24 h. In blocking experiments, CT26 cells were pretreated with NAC for 2 h and then stimulated with SK. **A** ROS generation in CT26 cells were indicated by the green fluorescence of 2',7'-dichlorofluorescein (DCF) that was

oxidized from 2',7'-dichlorodihydrofluorescein diacetate (H₂DCFDA) by ROS. **B, C** Western blot analyses for expression of Hsp70 in CT26 cells treated with SK or/and NAC. β -actin was used as a loading control. Data are expressed as mean \pm SD of three independent experiments. **** P < 0.0001

Using the Hsp70^{-/-} mouse model, Dodd et al. proved that Hsp70 played a key role in tumor recognition by adaptive immune system and in facilitating anti-tumor immunity. Also, Hsp70^{-/-} tumors exhibits significant reduction in the infiltration of immune cells [34]. In addition, Tsang et al. found that the immunogenicity of CT26 cell was mainly dependent on the release of Hsp70 [35]. Komarova et al. also proved that Hsp70-containing extracellular vesicles could cause full-scale antitumor effect in CT-26 cells by activating of adaptive immunity [36]. In our experiment, we also have observed that SK could significant upregulate the expression of Hsp70 in CT26 cells, suggesting Hsp70

might play a critical role in SK-induced immune activation, and further enhanced the efficacy of PD-1 blockade in CT26 tumor-bearing mouse model. Majority of research have demonstrated that ROS production and ER stress both produced DAMPs to induce tumor cells death [10–13, 37]. In our study, we also found that the expression of Hsp70 was induced by increased ROS after SK treatments, indicating that ROS was a potential inducer of CT26 cell death upon treatment with SK. Besides, we have found that silencing of PKM2 in CT26 cells reverts ROS upregulation induced by SK, indicating that increased ROS was induced by SK in a PKM2-dependent manner.

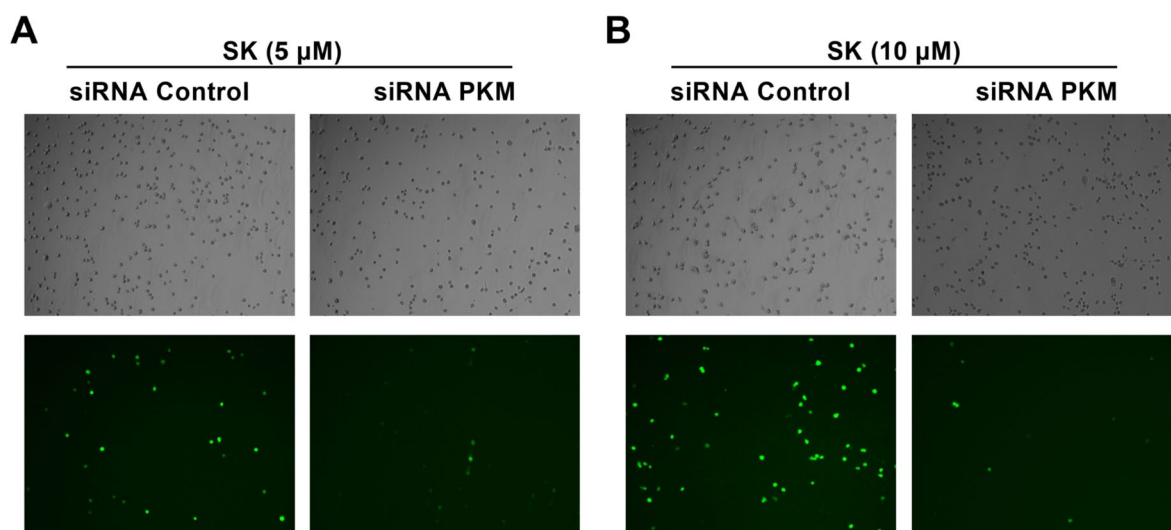


Fig. 4 Silencing of PKM2 in CT26 cells reverts ROS upregulation induced by Shikonin. CT26 cells were transfected with a small interference oligonucleotide against PKM2 (20 μ M) for 48 h, and then CT26 cells were incubated with SK at 5 μ M (A) or 10 μ M (B) for 12

h. The generation of ROS was determined by measuring the intensity of green fluorescence of 2',7'-dichlorofluorescein (DCF). Data are from one of three independent experiments

Fig. 5 Shikonin synergizes with PD-1 blockade in CT26 tumor mice model. (A) Experimental design for the treatment in CT26 tumor-bearing mice. 6×10^5 CT26 cells were subcutaneously inoculated into BALB/c mice in the right inguinal region. Tumor-bearing mice were randomized into 4 groups: Group A: IgG (n=5); Group B: IgG+SK (n=5); Group C: anti-PD-1 mAb (n=5); Group D: anti-PD-1 mAb+SK (n=5). Mice were given drugs when the tumor volume grew to about 62.5 mm^3 . SK or DMSO control was intraperitoneally injected at 3 mg/kg every two days for a total of seven times. Anti-PD-1 antibody or IgG control was intraperitoneally injected at 50 μ g/mice on the 5th and 9th day. (B) Growth curves of CT26 tumors were measured after treatment with SK combined with α PD-1. Data are expressed as mean \pm SD. ****P < 0.0001

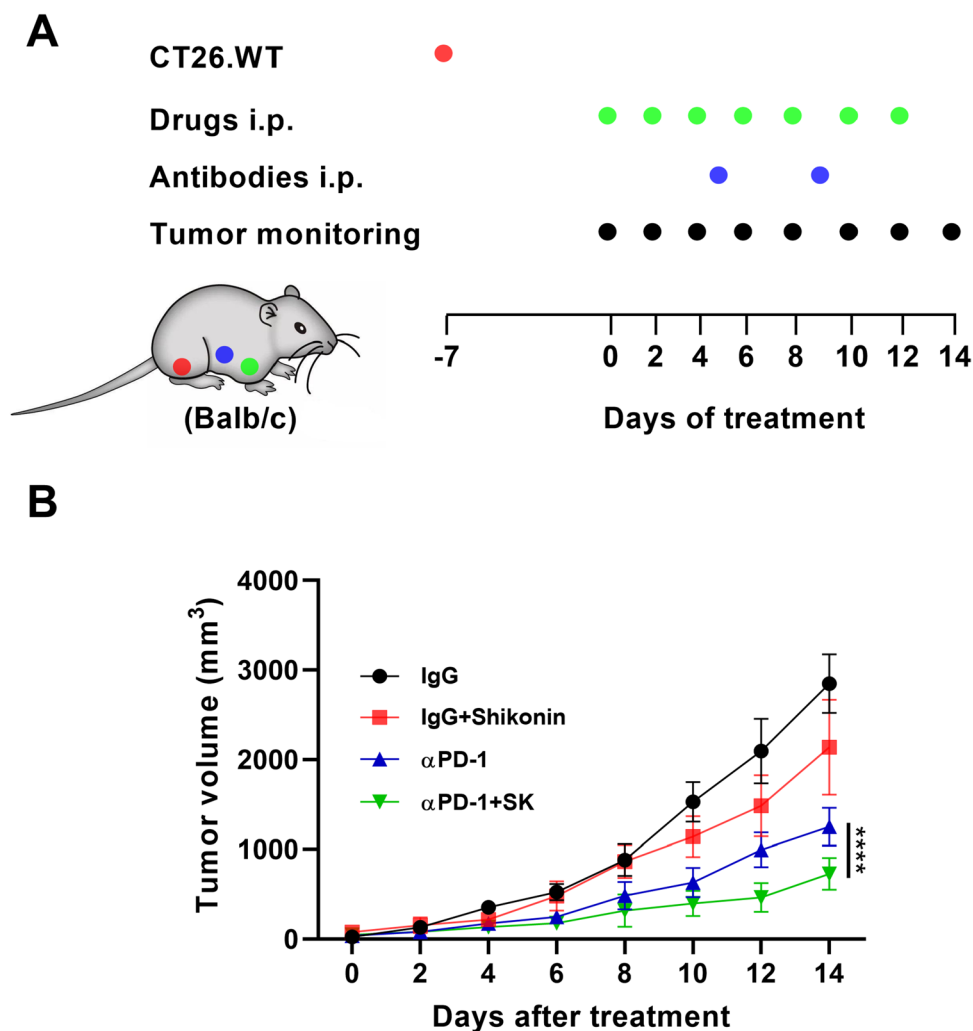
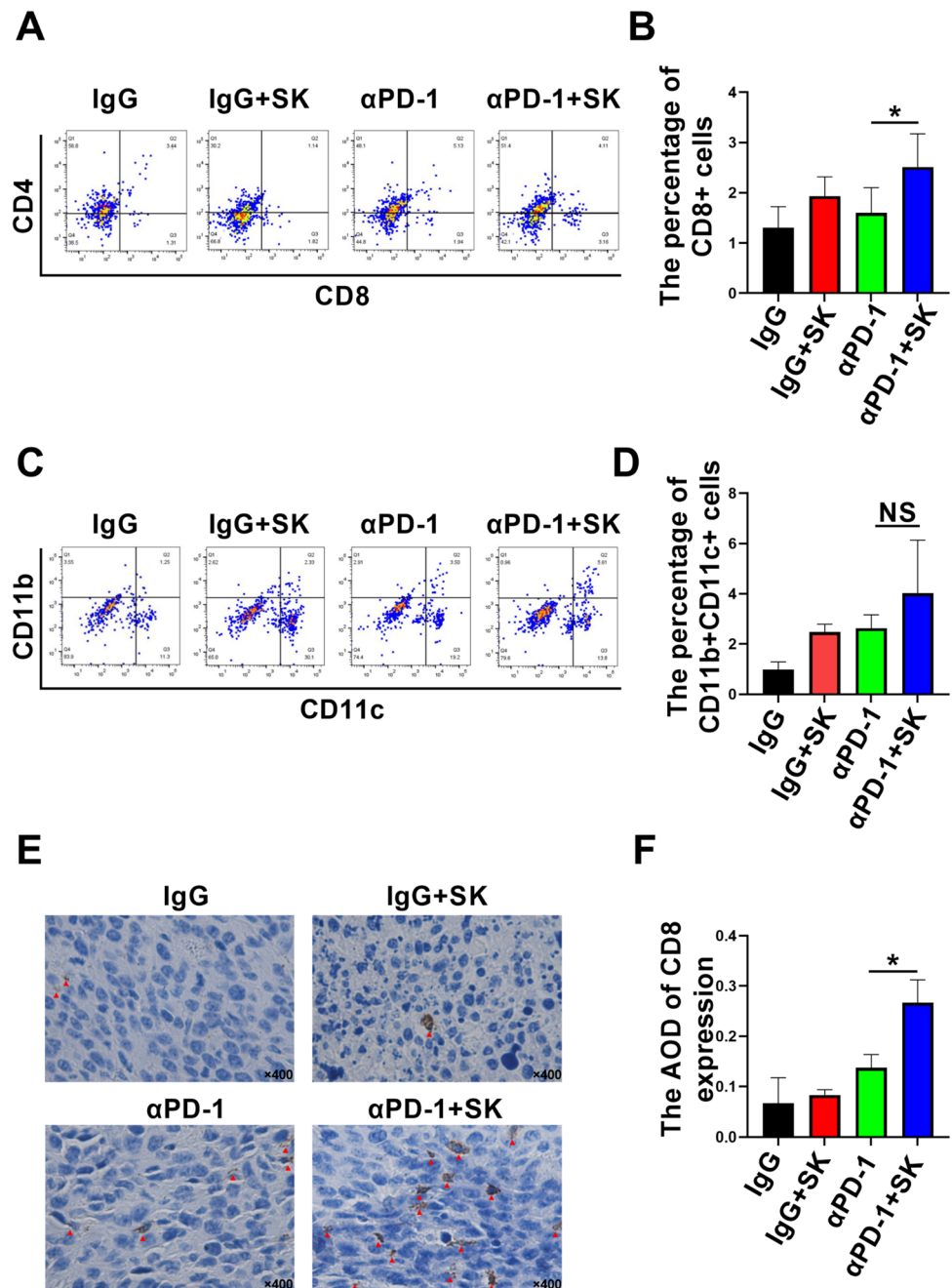


Fig. 6 Combinational Shikonin and PD-1 blockade modified tumor immune microenvironment. Immune microenvironment in solid tumor was evaluated and the percentage of intratumoral T or DC cells were determined by using flow cytometry. The percentages of intratumoral CD8⁺T cells (A, B) and CD11b⁺CD11c⁺ cells (C, D) were analyzed by flow cytometry after treatments. CD8⁺T cell in tumor was also evaluated using immunohistochemistry. E, F The average optical density (AOD) of CD8⁺T cells was shown and data are expressed as mean \pm SD. *P < 0.05



Our research findings those SK improves the effectiveness of PD-1 blockade in colorectal cancer are consistent with those of Wang et al. [20]. In their study, the authors found that SK and BET inhibitor JQ1 which downregulate PD-L1 expression in tumor cells instead of directly blocking the binding between PD-1 and PD-L1 can synergistically inhibit tumor growth by activating ICD, repolarizing TAM2 and inhibiting glycolysis.

In summary, our study shows that the combination of SK and anti-PD-1 mAb is a potential therapeutic strategy for MSS colorectal cancer. SK is a promising drug candidate for cancer immunotherapy. Until now, SK has not been utilized for prevention or clinical therapy due to its similarity with chemotherapeutic drugs, which can potentially result in side effects. Further research efforts should be directed towards developing a carrier that can accurately deliver SK to tumor tissues.

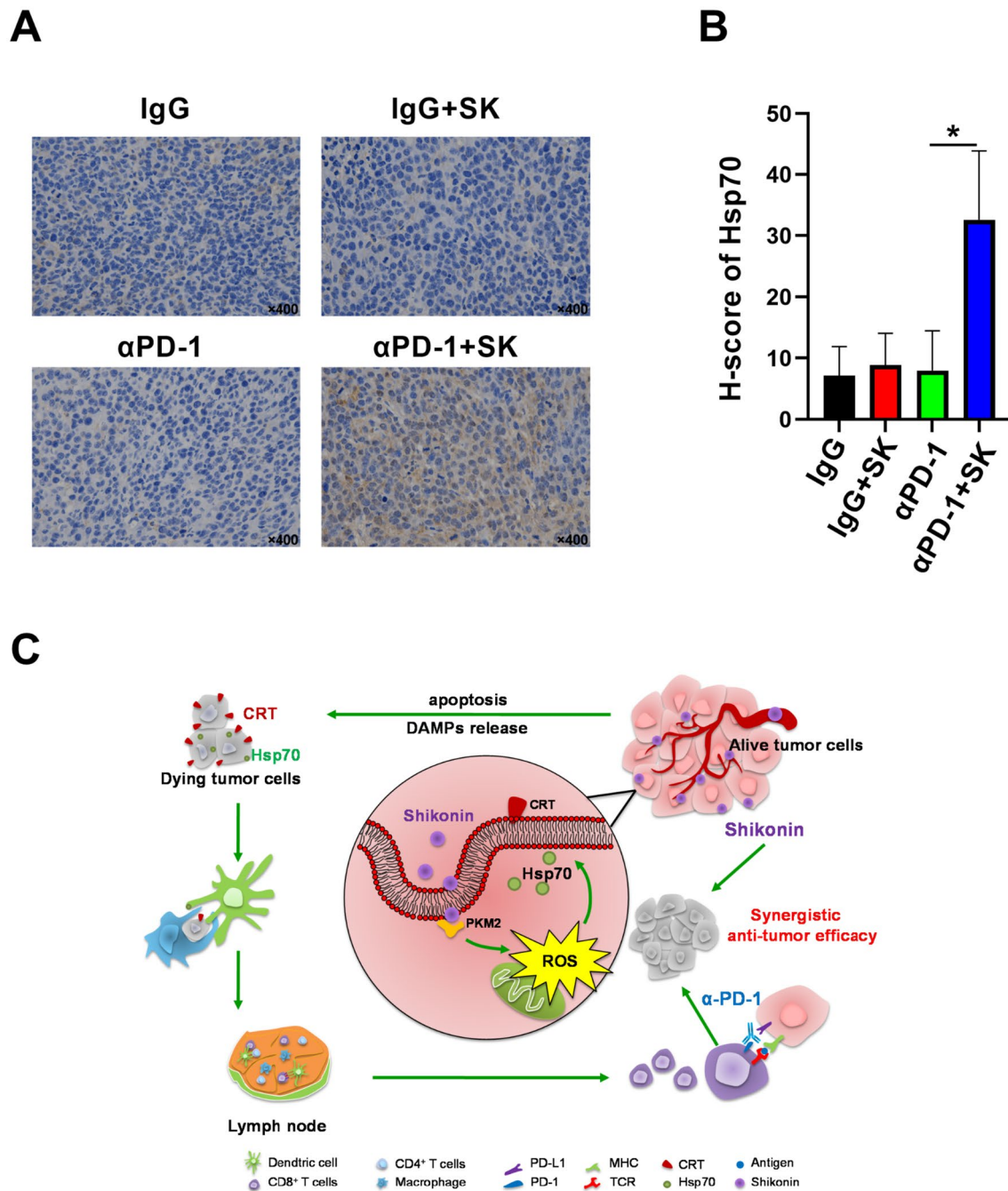


Fig. 7 The cellular and molecular mechanism underlying the synergistic effect of αPD-1 and SK in CT26 tumor mice model. **A** Hsp70 expression in tumor was determined using immunohistochemistry. **B** H-score of Hsp70 in tumor was shown and data are expressed as mean ± SD of three independent experiments. * $P < 0.05$. **C** Anti-tumor mechanism underlying the synergistic effect of αPD-1 and SK. Shikonin could synergize with PD-1 blockade in CT26 tumor model,

along with increased CD8⁺ T cells and DC cells. CT26 cell death was induced by SK via classically programmed and immunogenic pathways. Among three DAMPs, SK specifically induced Hsp70 upregulation dependent on increased ROS, whilst silencing of PKM2 in CT26 cells reverses ROS upregulation. Our study elucidated the potential role of ‘Shikonin-PKM2-ROS-Hsp70’ axis in the promotion of efficacy of PD-1 blockade in CRC treatments

Conclusions

Shikonin and PD-1 blockade produced synergistic antitumor effects in CT26 tumor-bearing mouse model by upregulating

the expression of Hsp70. Our study elucidated the potential role of ‘Shikonin-PKM2-ROS-Hsp70’ axis in the promotion of efficacy of PD-1 blockade, providing a potential strategy and targets for CRC treatments.

Author contributions JHC, JL and QX were involved in the design of the experiments and drafted the manuscript. JL, XLL and XMW were involved in data analysis and editing of the manuscript. JL, JW and XY reviewed and edited the manuscript. YL was involved in the design of the experiments, data analysis, and reviewed and edited the manuscript. All authors read and approved the final manuscript.

Funding This work was supported by the [Shandong Provincial Natural Science Foundation] under Grant [ZR2022MH207]; [the Major Science and Technology Innovation Project of Shandong Province] under Grant [2018CXGC1220]; [Traditional Chinese Medicine Science and Technology Development Plan of Shandong Province] under Grant [2019–0377]; [Shandong Provincial Qianfoshan Hospital] under Grant [QYPY2020NSFC1015, QYPY2020NSFC0821].

Data availability The authors confirm that the data supporting the findings of this study are available within the article.

Declarations

Conflict of interest The authors report no conflict of interest.

Ethical approval All animal experiment has been approved by the Ethics Committee of the first affiliated Hospital of Shandong first Medical University.

Open Access This article is licensed under a Creative Commons Attribution 4.0 International License, which permits use, sharing, adaptation, distribution and reproduction in any medium or format, as long as you give appropriate credit to the original author(s) and the source, provide a link to the Creative Commons licence, and indicate if changes were made. The images or other third party material in this article are included in the article's Creative Commons licence, unless indicated otherwise in a credit line to the material. If material is not included in the article's Creative Commons licence and your intended use is not permitted by statutory regulation or exceeds the permitted use, you will need to obtain permission directly from the copyright holder. To view a copy of this licence, visit <http://creativecommons.org/licenses/by/4.0/>.

References

1. Torre LA, Bray F, Siegel RL, Ferlay J, Lortet-Tieulent J, Jemal A (2015) Global cancer statistics 2012. *Cancer J Clin* 65(2):87–108. <https://doi.org/10.3322/caac.21262>
2. Damato A, Bergamo F, Antonuzzo L, Nasti G, Iachetta F, Romagnani A, Gervasi E, Larocca M, Pinto C (2021) FOLFOXIRI/bevacizumab plus nivolumab as first-line treatment in metastatic colorectal cancer RAS/BRAF mutated: safety run-in of phase II NIVACOR trial. *Front Oncol* 11:766500. <https://doi.org/10.3389/fonc.2021.766500>
3. Provenzale D, Ness RM, Llor X, Weiss JM, Abbadessa B, Cooper G, Early DS, Friedman M, Giardiello FM, Glaser K, Gurudu S, Halverson AL, Issaka R, Jain R, Kanth P, Kidambi T, Lazenby AJ, Maguire L, Markowitz AJ, May FP, Ogba N (2020) NCCN guidelines insights: colorectal cancer screening, version 2.2020. *J Natl Compr Cancer Netw* 18(10):1312–1320. <https://doi.org/10.6004/jnccn.2020.0048>
4. Ascierto PA, Del Vecchio M, Mandalá M, Gogas H, Arance AM, Dalle S, Cowey CL, Schenker M, Grob JJ, Chiarion-Sileni V, Márquez-Rodas I, Butler MO, Maio M, Middleton MR, de la Cruz-Merino L, Arenberger P, Atkinson V, Hill A, Fecher LA, Millward M, Weber J (2020) Adjuvant nivolumab versus ipilimumab in resected stage IIIB–C and stage IV melanoma (CheckMate 238): 4-year results from a multicentre, double-blind, randomised, controlled, phase 3 trial. *Lancet Oncol* 21(11):1465–1477. [https://doi.org/10.1016/S1470-2045\(20\)30494-0](https://doi.org/10.1016/S1470-2045(20)30494-0)
5. Mok TSK, Wu YL, Kudaba I, Kowalski DM, Cho BC, Turna HZ, Castro G Jr, Srimuninnimit V, Laktionov KK, Bondarenko I, Kubota K, Lubiniecki GM, Zhang J, Kush D, Lopes G, KEYNOTE-042 Investigators (2019) Pembrolizumab versus chemotherapy for previously untreated, PD-L1-expressing, locally advanced or metastatic non-small-cell lung cancer (KEYNOTE-042): a randomised, open-label, controlled, phase 3 trial. *Lancet* 393(10183):1819–1830. [https://doi.org/10.1016/S0140-6736\(18\)32409-7](https://doi.org/10.1016/S0140-6736(18)32409-7)
6. Overman MJ, McDermott R, Leach JL, Lonardi S, Lenz HJ, Morse MA, Desai J, Hill A, Axelson M, Moss RA, Goldberg MV, Cao ZA, Ledezine JM, Maglinte GA, Kopetz S, André T (2017) Nivolumab in patients with metastatic DNA mismatch repair-deficient or microsatellite instability-high colorectal cancer (CheckMate 142): an open-label, multicentre, phase 2 study. *Lancet Oncol* 18(9):1182–1191. [https://doi.org/10.1016/S1470-2045\(17\)30422-9](https://doi.org/10.1016/S1470-2045(17)30422-9)
7. André T, Shiu KK, Kim TW, Jensen BV, Jensen LH, Punt C, Smith D, Garcia-Carbonero R, Benavides M, Gibbs P, de la Fouchardiere C, Rivera F, Elez E, Bendell J, Le DT, Yoshino T, Van Cutsem E, Yang P, Farooqui MZH, Marinello P, KEYNOTE-177 Investigators (2020) Pembrolizumab in microsatellite-instability-high advanced colorectal cancer. *New Engl J Med* 383(23):2207–2218. <https://doi.org/10.1056/NEJMoa2017699>
8. Stein A, Folprecht G (2018) Immunotherapy of colon cancer. *Oncol Res Treat* 41(5):282–285. <https://doi.org/10.1159/000488918>
9. Tang D, Kang R, Coyne CB, Zeh HJ, Lotze MT (2012) PAMPs and DAMPs: signal 0s that spur autophagy and immunity. *Immunol Rev* 249(1):158–175. <https://doi.org/10.1111/j.1600-065X.2012.01146.x>
10. Green DR, Ferguson T, Zitvogel L, Kroemer G (2009) Immunogenic and tolerogenic cell death. *Nat Rev Immunol* 9(5):353–363. <https://doi.org/10.1038/nri2545>
11. Tesniere A, Schlemmer F, Boige V, Kepp O, Martins I, Ghiringhelli F, Aymeric L, Michaud M, Apetoh L, Barault L, Mendiboure J, Pignon JP, Jooste V, van Endert P, Ducreux M, Zitvogel L, Piard F, Kroemer G (2010) Immunogenic death of colon cancer cells treated with oxaliplatin. *Oncogene* 29(4):482–491. <https://doi.org/10.1038/onc.2009.356>
12. Zitvogel L, Kepp O, Senovilla L, Menger L, Chaput N, Kroemer G (2010) Immunogenic tumor cell death for optimal anti-cancer therapy: the calreticulin exposure pathway. *Clin Cancer Res* 16(12):3100–3104. <https://doi.org/10.1158/1078-0432.CCR-09-2891>
13. Obeid M, Tesniere A, Ghiringhelli F, Fimia GM, Apetoh L, Perfettini JL, Castedo M, Mignot G, Panaretakis T, Casares N, Métivier D, Larochette N, van Endert P, Ciccosanti F, Piacentini M, Zitvogel L, Kroemer G (2007) Calreticulin exposure dictates the immunogenicity of cancer cell death. *Nat Med* 13(1):54–61. <https://doi.org/10.1038/nm1523>
14. Boulous JC, Rahama M, Hegazy MF, Efferth T (2019) Shikonin derivatives for cancer prevention and therapy. *Cancer Lett* 459:248–267. <https://doi.org/10.1016/j.canlet.2019.04.033>
15. Chandimali N, Sun HN, Kong LZ, Zhen X, Liu R, Kwon T, Lee DS (2019) Shikonin-induced apoptosis of colon cancer cells is reduced by peroxiredoxin V expression. *Anticancer Res* 39(11):6115–6123. <https://doi.org/10.21873/anticancer.13819>
16. Zhu J, Zhao L, Luo B, Sheng W (2019) Shikonin regulates invasion and autophagy of cultured colon cancer cells by inhibiting yes-associated protein. *Oncol Lett* 18(6):6117–6125. <https://doi.org/10.3892/ol.2019.10980>

17. He G, He G, Zhou R, Pi Z, Zhu T, Jiang L, Xie Y (2016) Enhancement of cisplatin-induced colon cancer cells apoptosis by shikonin, a natural inducer of ROS in vitro and in vivo. *Biochem Biophys Res Commun* 469(4):1075–1082. <https://doi.org/10.1016/j.bbrc.2015.12.100>
18. Lin TJ, Lin HT, Chang WT, Mitapalli SP, Hsiao PW, Yin SY, Yang NS (2015) Shikonin-enhanced cell immunogenicity of tumor vaccine is mediated by the differential effects of DAMP components. *Mol Cancer* 14:174. <https://doi.org/10.1186/s12943-015-0435-9>
19. Chen HM, Wang PH, Chen SS, Wen CC, Chen YH, Yang WC, Yang NS (2012) Shikonin induces immunogenic cell death in tumor cells and enhances dendritic cell-based cancer vaccine. *Cancer Immunol Immunother* 61(11):1989–2002. <https://doi.org/10.1007/s00262-012-1258-9>
20. Wang H, Tang Y, Fang Y, Zhang M, Wang H, He Z, Wang B, Xu Q, Huang Y (2019) Reprogramming tumor immune microenvironment (TIME) and metabolism via biomimetic targeting codelivery of shikonin/JQ1. *Nano Lett* 19(5):2935–2944. <https://doi.org/10.1021/acs.nanolett.9b00021>
21. Yang Q, Ji M, Guan H, Shi B, Hou P (2013) Shikonin inhibits thyroid cancer cell growth and invasiveness through targeting major signaling pathways. *J Clin Endocrinol Metab* 98(12):E1909–E1917. <https://doi.org/10.1210/jc.2013-2583>
22. Li W, Liu J, Jackson K, Shi R, Zhao Y (2014) Sensitizing the therapeutic efficacy of taxol with shikonin in human breast cancer cells. *PLoS One* 9(4):e94079. <https://doi.org/10.1371/journal.pone.0094079>
23. Ajona D, Ortiz-Espinosa S, Moreno H, Lozano T, Pajares MJ, Agorreta J, Bértolo C, Lasarte JJ, Vicent S, Hoehlig K, Vater A, Lecanda F, Montuenga LM, Pio R (2017) A combined PD-1/C5a blockade synergistically protects against lung cancer growth and metastasis. *Cancer Discov* 7(7):694–703. <https://doi.org/10.1158/2159-8290.CD-16-1184>
24. Llopiz D, Ruiz M, Villanueva L, Iglesias T, Silva L, Egea J, Lasarte JJ, Pivette P, Trochon-Joseph V, Vasseur B, Dixon G, Sangro B, Sarobe P (2019) Enhanced anti-tumor efficacy of checkpoint inhibitors in combination with the histone deacetylase inhibitor belinostat in a murine hepatocellular carcinoma model. *Cancer Immunol Immunother* 68(3):379–393. <https://doi.org/10.1007/s00262-018-2283-0>
25. Guo R, Zhang L, Meng J (2020) Circular RNA ANKRD36 attends to lipopolysaccharide-aroused MRC-5 cell injury via regulating microRNA-31-3p. *Biofactors* 46(3):391–401. <https://doi.org/10.1002/biof.1592>
26. Zhang H, Gong W, Wu S, Perrett S (2022) Hsp70 in Redox homeostasis. *Cells* 11(5):829. <https://doi.org/10.3390/cells11050829>
27. Yang P, Li Z, Fu R, Wu H, Li Z (2014) Pyruvate kinase M2 facilitates colon cancer cell migration via the modulation of STAT3 signalling. *Cell Signal* 26(9):1853–1862. <https://doi.org/10.1016/j.cellsig.2014.03.020>
28. Zhou CF, Li XB, Sun H, Zhang B, Han YS, Jiang Y, Zhuang QL, Fang J, Wu GH (2012) Pyruvate kinase type M2 is upregulated in colorectal cancer and promotes proliferation and migration of colon cancer cells. *IUBMB Life* 64(9):775–782. <https://doi.org/10.1002/iub.1066>
29. Zheng D, Jiang Y, Qu C, Yuan H, Hu K, He L, Chen P, Li J, Tu M, Lin L, Chen H, Lin Z, Lin W, Fan J, Cheng G, Hong J (2020) Pyruvate kinase M2 tetramerization protects against hepatic stellate cell activation and liver fibrosis. *Am J Pathol* 190(11):2267–2281. <https://doi.org/10.1016/j.ajpath.2020.08.002>
30. Limagne E, Thibaudin M, Nuttin L, Spill A, Derangère V, Fumet JD, Amellal N, Peranzoni E, Cattani V, Ghiringhelli F (2019) Trifluridine/tipiracil plus oxaliplatin improves PD-1 blockade in colorectal cancer by inducing immunogenic cell death and depleting macrophages. *Cancer Immunol Res* 7(12):1958–1969. <https://doi.org/10.1158/2326-6066.CIR-19-0228>
31. Larkin J, Chiarion-Sileni V, Gonzalez R, Grob JJ, Rutkowski P, Lao CD, Cowey CL, Schadendorf D, Wagstaff J, Dummer R, Ferrucci PF, Smylie M, Hogg D, Hill A, Márquez-Rodas I, Haanen J, Guidoboni M, Maio M, Schöffski P, Carlino MS, Wolchok JD (2019) Five-year survival with combined nivolumab and Ipilimumab in advanced melanoma. *New Engl J Med* 381(16):1535–1546. <https://doi.org/10.1056/NEJMoa1910836>
32. Lee CH, Shah AY, Rasco D, Rao A, Taylor MH, Di Simone C, Hsieh JJ, Pinto A, Shaffer DR, Girones Sarrio R, Cohn AL, Vogelzang NJ, Bilen MA, Gunnestad Ribe S, Goksel M, Tennøe ØK, Richards D, Sweis RF, Courtright J, Heinrich D, Motzer RJ (2021) Lenvatinib plus pembrolizumab in patients with either treatment-naïve or previously treated metastatic renal cell carcinoma (study 111/KEYNOTE-146): a phase 1b/2 study. *Lancet Oncol* 22(7):946–958. [https://doi.org/10.1016/S1470-2045\(21\)00241-2](https://doi.org/10.1016/S1470-2045(21)00241-2)
33. Reck M, Rodríguez-Abreu D, Robinson AG, Hui R, Csőszi T, Fülöp A, Gottfried M, Peled N, Tafreshi A, Cuffe S, O'Brien M, Rao S, Hotta K, Leal TA, Riess JW, Jensen E, Zhao B, Pietanza MC, Brahmer JR (2021) Five-year outcomes with pembrolizumab versus chemotherapy for metastatic non-small-cell lung cancer with PD-L1 tumor proportion score ≥ 50 . *J Clin Oncol* 39(21):2339–2349. <https://doi.org/10.1200/JCO.21.00174>
34. Dodd K, Nance S, Quezada M, Janke L, Morrison JB, Williams RT, Beere HM (2015) Tumor-derived inducible heat-shock protein 70 (HSP70) is an essential component of anti-tumor immunity. *Oncogene* 34(10):1312–1322. <https://doi.org/10.1038/nc.2014.63>
35. Tsang YW, Huang CC, Yang KL, Chi MS, Chiang HC, Wang YS, Andocs G, Szasz A, Li WT, Chi KH (2015) Improving immunological tumor microenvironment using electro-hyperthermia followed by dendritic cell immunotherapy. *BMC Cancer* 15:708. <https://doi.org/10.1186/s12885-015-1690-2>
36. Komarova EY, Suezov RV, Nikotina AD, Aksenov ND, Garaeva LA, Shtam TA, Zhakhov AV, Martynova MG, Bystrova OA, Istomina MS, Ischenko AM, Margulis BA, Guzhova IV (2021) Hsp70-containing extracellular vesicles are capable of activating of adaptive immunity in models of mouse melanoma and colon carcinoma. *Sci Rep* 11(1):21314. <https://doi.org/10.1038/s41598-021-00734-4>
37. Ghiringhelli F, Apetoh L, Tesniere A, Aymeric L, Ma Y, Ortiz C, Vermaelen K, Panaretakis T, Mignot G, Ullrich E, Perfettini JL, Schlemmer F, Tasdemir E, Uhl M, Génin P, Civas A, Ryffel B, Kanellopoulos J, Tschopp J, André F, Zitvogel L (2009) Activation of the NLRP3 inflammasome in dendritic cells induces IL-1 β -dependent adaptive immunity against tumors. *Nat Med* 15(10):1170–1178. <https://doi.org/10.1038/nm.2028>

Publisher's Note Springer Nature remains neutral with regard to jurisdictional claims in published maps and institutional affiliations.